

FIP: Endowing Robust Motion Capture on Daily Garment by Fusing Flex and Inertial Sensors

Jiawei Fang*
jiaweif@stu.xmu.edu.cn
Xiamen University
Xiamen, China

Xiaoxia Gao
gaoxiaoxia@stu.xmu.edu.cn
Xiamen University
Xiamen, China

Ruonan Zheng*
30920241154558@stu.xmu.edu.cn
Xiamen University
Xiamen, China

Chengxu Zuo
zuochengxu@stu.xmu.edu.cn
Xiamen University
Xiamen, China

Yiyue Luo
yiyueluo@mit.edu
MIT CSAIL
Cambridge, Massachusetts, USA

Yuan Yao
furtheryao@stu.xmu.edu.cn
Xiamen University
Xiamen, China

Shihui Guo[†]
guoshihui@xmu.edu.cn
Xiamen University
Xiamen, China



Figure 1: FIP endows real-time, accurate motion capture on daily clothes by fusing flex and inertial sensors.

Abstract

What if our clothes could capture our body motion accurately? This paper introduces Flexible Inertial Poser (FIP), a novel motion-capturing system using daily garments with two elbow-attached flex sensors and four Inertial Measurement Units (IMUs). To address the inevitable sensor displacements in loose wearables which degrade joint tracking accuracy significantly, we identify the distinct characteristics of the flex and inertial sensor displacements and develop a Displacement Latent Diffusion Model and a Physics-informed Calibrator to compensate for sensor displacements based on such observations, resulting in a substantial improvement in motion capture accuracy. We also introduce a Pose Fusion Predictor to enhance multimodal sensor fusion. Extensive experiments demonstrate that our method achieves robust performance across varying

body shapes and motions, significantly outperforming SOTA IMU approaches with a 19.5% improvement in angular error, a 26.4% improvement in elbow angular error, and a 30.1% improvement in positional error. FIP opens up opportunities for ubiquitous human-computer interactions and diverse interactive applications such as Metaverse, rehabilitation, and fitness analysis. Our project page can be seen at [Flexible Inertial Poser](#).

CCS Concepts

• Human-centered computing → Ubiquitous and mobile computing.

Keywords

Motion Capture, Wearable Computers, Sensor Fusion

*Both authors contributed equally to this research.

[†]Corresponding Author.

ACM Reference Format:

Jiawei Fang, Ruonan Zheng, Yuan Yao, Xiaoxia Gao, Chengxu Zuo, Shihui Guo, and Yiyue Luo. 2025. FIP: Endowing Robust Motion Capture on Daily Garment by Fusing Flex and Inertial Sensors. In *Proceedings of the 2025 CHI Conference on Human Factors in Computing Systems (CHI '25)*, April 26-May 1, 2025, Yokohama, Japan. ACM, New York, NY, USA, 15 pages. <https://doi.org/XXXXXXX>

1 Introduction

Human motion capture (MoCap) has emerged as a pivotal technology in fields such as animation, movie production, and virtual/augmented reality. Wearable motion capture offers advantages in portability, privacy friendliness, and robustness against extreme lighting and occlusion, compared to marker and vision-based approaches [35, 83]. Inertial and flex sensors become the *de facto* SOTA sensing mechanism that people use for wearable MoCap. Inertial sensors, also known as Inertial Measurement Units (IMUs), provide an efficient and compact means of measuring the orientation and acceleration of the human skeleton with the leading advantage of accuracy. Recent works achieve posture estimation with a sparse number (3-6) of IMUs [19, 21, 74, 76, 77]. However, this method requires IMUs to be tightly attached to the body for stable measurement, which inevitably produces an uncomfortable wearing experience, and results in significant measurement errors due to the underconstrained nature of joints such as elbows and knees.

Flex sensors, also known as bending sensors, accurately measure the degree of flexion in elbow and knee joints [8, 13, 87] by leveraging diverse sensing mechanisms, such as resistive, capacitive, and inductive sensing. They are lightweight, biocompatible, and flexible [44, 57], offering solutions to the limitations posed by sparse IMU setups and enhancing measurement accuracy without compromising user comfortableness. This motivates the fusion of flex sensors and IMUs in daily garments for *Clothes-based MoCap*, harnessing the strengths of each to create a more effective and comfortable MoCap solution.

However, *Clothes-based MoCap* must overcome the critical sensor displacements challenges [2, 3] before it can be effectively used for real-world human-computer interaction (HCI) applications [88]. We observe two main sensor displacements arising from the loose-fitting clothing: *Primary Displacement* occurs when users first put on the clothing, causing significant position shift relative to the human body due to substantial body-fabric interaction whereas *Real-time Displacement* happens as the sensors move and vibrate with the loose-fitting clothing. Generally, the performance of flex sensors is significantly affected by *Primary Displacement*. In contrast, *Inertial-based MoCap* usually mitigates the Primary Displacement through T-pose calibration [54, 76], leaving *Real-time Displacement* the dominant factor.

To this end, this paper introduces Flexible Inertial Poser (FIP), a *Clothes-based MoCap* solution that achieves both robust and comfortable pose estimation with multi-modal sensor fusion (Fig. 1). By integrating four IMUs and two auxiliary flex sensors into a loose-fitting garment, FIP leverages the unique advantages of both sensor types, offering significant advancement in accuracy, accessibility, and comfort. To address the sensor displacements based on each unique sensor type, FIP includes three components: 1) a **Displacement Latent Diffusion Model** to synthesize sensor disturbance in various conditions, addressing the *Real-time Displacement* of IMUs; 2) a **Physics-informed Calibrator** to register data in different wearing condition, addressing the *Primary Displacement* of flex sensors; 3) a **Pose Fusion Predictor** to fuse multi-modal sensor readings for pose estimation. To validate our approach, we collected

a real-world testing dataset from ten users with ten different expressive motions. Extensive experimental results demonstrated the effectiveness of our method. Our work represents a beginning in exploring multi-modal sensor fusion in loose clothing, paving the way for diverse interactive applications.

In conclusion, our main contributions are as follows:

- We develop a real-time, accurate method for human motion capture using loosely worn clothes embedded with a sparse number of IMUs and auxiliary flex sensors, ensuring both user comfort and high accuracy.
- We implement a novel **Displacement Latent Diffusion Model** for synthesizing inertial sensor data with *Real-time Displacement*, complemented by a **Physics-Informed Calibrator** that effectively addresses the *Primary Displacement* in flex sensors. In addition, a **Pose Fusion Predictor** to fuse multi-modal sensor readings for pose estimation.
- We evaluate our approach, which significantly reduces elbow tracking errors and achieves SOTA performance in overall joint motion capture, surpassing all competing approaches.
- We demonstrate our approach in Metaverse, rehabilitation, and fitness analysis, highlighting the benefits and potentials with *Clothes-based MoCap*.

2 Related Work

2.1 Motion Capture

Many applications such as gaming, bio-mechanical analysis, movie production, and emerging human-computer interaction paradigms such as Virtual and Augmented Reality (VR/AR) require a means to human motion capture (MoCap). Such applications impose three challenging constraints on pose reconstruction: (i) precise MoCap in real-time, (ii) work in everyday settings including in/outdoors and easy to access, (iii) minimally intrusive in terms of user experience [41, 76, 86].

We conducted a detailed discussion on the advantages and disadvantages of four different paradigms of MoCap methods, as outlined below, and summarized our findings in Fig. 2. In summary, previous methods relied on a single type of sensor, limiting the potential for accurate motion capture. In contrast, our method, FIP, integrates both IMUs and flex sensors into loose-fitting clothing, achieving both accuracy and comfort in motion capture.

2.1.1 Vision-based MoCap. Most commonly, the MoCap task is achieved using commercial marker-based systems like Vicon [65]. These systems [7, 15, 49] achieve high accuracy by tracking markers on the body. However, they require costly infrastructure and physical markers placed on users, limiting accessibility in everyday contexts. Markerless single RGB or RGB-D cameras methods have gained attraction [1, 12, 14, 28, 31, 33, 34, 40, 52, 56, 60, 71–73, 78–80], but similar to multi-camera systems [10, 30, 61, 70, 82], they are still highly sensitive to occlusions, lighting variations, and the actor’s appearance. Additionally, many of these assume a static camera setting, limiting capture space and reducing effectiveness in dynamic or outdoor environments. These constraints hinder the broader application of optical motion capture.

2.1.2 Inertial-based MoCap. Inertial Measurement Units (IMUs) provide efficient and compact measurement for the orientation and

acceleration of the human skeleton, facilitating accurate motion capture [23]. Commercial systems like Noitom [45] and Xsens [42] achieve precise capture by embedding dense IMU arrays into tight-fitting bandages. However, the intrusive nature of these setups significantly restricts user comfort and accessibility. To address these challenges, recent research has focused on sparse-IMU solutions to balance functionality and user comfort. SIP reduced the IMU count to six, but limited to offline [66]. DIP introduced real-time performance using deep recurrent neural networks, but was constrained to local pose estimations [19]. TransPose improved global translations by incorporating foot-ground contact constraints [76]. PIP [74] and TIP [21] refine TransPose further: PIP ensures physical plausibility through physics-based optimization, while TIP enhances tracking accuracy using transformer architectures. PNP [77] improved the accuracy and robustness by compensating for fictitious forces in non-inertial frames. Furthermore, UIP [?] combined IMUs with UWB to constrain drift and jitter, improving accuracy. IMUPoser [?] estimated pose by IMUs in devices like smartphones, smartwatches, and earbuds, eliminating the need for external sensors and further improving comfort and accessibility. However, its accuracy may decline when users lack or do not wear the required devices.

Despite these innovations, sparse-IMU systems still struggle with pose ambiguity, often misclassifying similar movements like sitting and standing, leading to errors in elbow and knee tracking. Moreover, they rely on tight straps for accuracy, compromising long-term comfort and wearability.

2.1.3 Flexible Sensor-based MoCap. Flexible sensors are emerging as promising solutions for long-term monitoring of human activities due to their insusceptibility to issues like lighting conditions, integration drift, or occlusions [29, 38, 44]. In addition, their inherent bio-compatibility, high stretchability, and lightweight design make them particularly suitable for monitoring of human physical status at extended duration, enhancing the overall user experience [36, 37]. Despite their comfort, flexible sensors may not yet match the precision of IMUs, as they are unable to directly measure the 3-axis orientation of bones, posing a less accurate full-body motion capture compared to inertial systems [9]. However, their strength of directly measuring joint angles through skin deformation, renders them particularly accurate for joints with noticeable deformation, such as the elbow [8, 22, 87] and knee joints [4, 50, 59].

In general, their seamless integration into clothing ensures enhanced comfort and long-term wearability. Although flexible sensors have not yet surpassed IMUs in full-body motion capture accuracy, their exceptional capabilities in tracking knee and elbow joints offer a promising complement to inertial MoCap systems, potentially enhancing both accuracy and user satisfaction.

2.1.4 Clothes-based MoCap. Clothing has been indispensable to everyday life since humans first donned garments for warmth and protection during the Ice Age [26]. In the modern world, the always-on nature and portability of clothing make it an ideal medium for interacting with digital realities [68]. Therefore, sensors are increasingly being embedded into garments to enable long-term MoCap. To obtain accurate data, mainstream approaches typically involve integrating either inertial sensors or flexible sensors at key joint locations within tight-fitting clothing. For instance, the

TESLASUIT incorporates a dense array of IMUs ($n=14$) into its tight-fitting garment [63]. On the other hand, Chen et al. demonstrate the use of six flexible sensors on an elbow pad to predict joint angles [8].

While tight-fitting clothing-based motion capture has shown promise, solutions for loose-fitting garments remain underexplored. LIP demonstrates robust accuracy by integrating a sparse set of IMUs ($n=4$) into a loose-fitting jacket [88], but its performance on the elbow joint is limited due to the sparse sensor placement. Other approaches, such as MoCaPose [85] and SeamPose [81], incorporate capacitive sensors into loose garments for motion capture. However, these methods rely on a single sensor type, restricting their accuracy and adaptability. In general, as shown in Tab. 1, our approach achieves accurate and comfortable motion capture paradigm at a smooth 60 Hz by leveraging both IMUs and flex sensors in everyday clothing. This multimodal integration is intuitive, as garments naturally serve as an ideal interface for sensor fusion.

Table 1: Comparison with other methods in loose-fitting clothing. Our FIP method demonstrates similar, or even superior, motion capture performance with higher frame rates.

Method	Sensor Types	FPS	Positional Error (cm)
MoCaPose	capacitive sensors	30*	8.80
SeamPose	capacitive sensors	30*	8.60
LIP	IMUs	30	9.99 ± 4.19
Ours	IMUs and flex sensors	60	8.06 ± 2.87

*: According to the dataset.

2.2 Algorithms for Sensor Displacements

Sensor displacements occur when sensors shift from their intended configuration, resulting in altered positioning that can challenge pre-trained pattern recognition models. To address this, researchers have employed transfer learning techniques [24, 53, 67], such as domain adaptation [6, 84] and self-supervised learning [11, 16, 20], to extract invariant features from displaced sensor data [27, 69]. For IMUs, static pose calibrations, like A-pose and T-pose [21, 45, 76], are commonly used to eliminate the initial relative rotation bias between the body and sensors, referred to as *Primary Displacement*. On another front, LIP generates synthetic loose IMU data to address *Real-time Displacement*. However, LIP relies on the assumption that the distributions of loose and tight IMU data are sufficiently similar, which may lead to the generated displacement distribution diverging from real-world conditions [88].

For flexible sensors, Zuo et al. proposed a self-adaptive algorithm that fine-tunes and aligns distributions to handle *Real-time Displacement* [87]. DisPad leverages fuzzy entropy to identify the closest matching distribution to the current displacement, effectively managing both circular and lateral sensor shifts [8]. Meanwhile, SuDA introduced a Sim2Real approach that aligns the support of source and target domains, rather than their distributions, achieving results comparable to supervised learning without the requirements for real labeled data [22].

To sum up, while these methods have been successful in addressing single-sensor displacement, handling displacement across



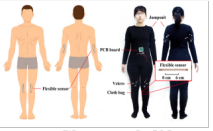


	Vision-based	Flexible Sensor-based	Inertial-based	Clothes-based	
Example	 Vicon [63]	 XNect [40]	 Chen et al. [9]	 PIP [72]	 FIP (Ours)
Accuracy	✓ Pricise MoCap system	✓ High accuracy when no occlusion	✗ Susceptible to sensor displacement, aging etc.	✓ High accuracy	✓ High accuracy
Comforts	✗ Tight-fitting clothes attached with markers	○ N/A	✓ Comfort; long-term track	✗ Tight-wearing	✓ Loose-wearing in daily garment
Accessibility	✗ Expensive (Over \$200K); hard to employ; only work indoors	✗ Fail when heavy occlusion, extreme weather, etc.	✓ Easy-to-wear; unperceivable	✗ Require a cumbersome wearing & calibration process (~1min)	✓ Unperceivable; fast wearing & calibration (~6s)

Figure 2: Comparison of related MoCap methods.

multiple sensors remains a significant challenge. In this work, we propose targeted algorithms for both flex and inertial sensors, designed to account for their distinct displacement characteristics and ensure robust performance in everyday garments.

2.3 Generative AI

Generative AI has widespread applications across various fields, including image [46, 48], speech [5], and text generation [47], with profound impact on the Human-Computer Interaction (HCI) community [43]. Variational Autoencoders (VAEs) [25] and Diffusion Models (DMs) [17], both of which are designed to learn underlying data distributions and generate new samples from them.

For VAEs, the model optimizes the Evidence Lower Bound (ELBO), formulated as:

$$\mathcal{L}(\xi, \phi; x) = \mathbb{E}_{q_{\phi}(z|x)} [\log p_{\xi}(x|z)] - D_{KL}(q_{\phi}(z|x) \parallel p(z)), \quad (1)$$

where $q_{\phi}(z|x)$ is the approximate posterior, $p_{\xi}(x|z)$ is the likelihood of generating the data, and D_{KL} is the Kullback-Leibler divergence that regularizes the latent space to follow a prior distribution.

Diffusion Models, in contrast, work by modeling the reverse process of a gradual noise addition. The forward process adds Gaussian noise to the data over T timesteps, modeled as:

$$q(x_t|x_{t-1}) = \mathcal{N}(x_t; \sqrt{1 - \beta_t}x_{t-1}, \beta_t I) \quad (2)$$

where β_t controls the noise schedule. The model learns the reverse process, recovering the original data by predicting the noise at each step:

$$p_{\theta}(x_{t-1}|x_t) = \mathcal{N}(x_{t-1}; \mu_{\theta}(x_t, t), \Sigma_{\theta}(x_t, t)) \quad (3)$$

By minimizing the difference between the added noise and the predicted noise, the model can generate data by starting from pure noise and iteratively denoising it.

Both VAEs and Diffusion Models are pivotal techniques in generative AI, driving advancements in generating high-quality, complex data across various domains. In our application, we seek to harness the capabilities of generative AI to create a diverse range of IMU displacements, which could enhance the robustness of pose estimation models.

3 Design & Prototyping of FIP

As shown in Fig. 3, our system prototype incorporates two flex sensors provided by Nitto¹ and four Xsens² MTI-3 IMUs into a jacket, endowing it with the ability for robust motion capture. The four IMUs are strategically placed on the left forearm, right forearm, back, and waist, while the two flex sensors are positioned at the left and right elbow. These sensors are connected with flexible wire and seamlessly integrated into the fabric through heat pressing, ensuring a non-invasive experience.



Figure 3: Prototype of the garment integrated with flex sensors, IMUs, and circuit board: (a-b) Front and back views of the garment, (c) IMU and circuit board positioned on the back, (d) IMU located at the waist, (e) Flexible sensors placed on the elbows and IMUs attached to the forearms.

3.1 Design

Our design prioritizes both user comfort and data collection accuracy. Sensor placement and readout interfaces are meticulously selected based on joint movement characteristics for effective integration.

Sensor Placement. Drawing on previous research, we positioned four IMUs at key joints with three degrees of freedom: the left forearm, right forearm, back, and waist. Given that the elbow has only one degree of freedom and rigid sensors could compromise comfort, we incorporated flexible bending sensors at the elbows of both sleeves to enhance tracking accuracy.

¹<https://www.nitto.com/>

²<https://www.xsens.com/>

Circuit Design. The sensor readout system comprises three components: the main control board, flex sensor connection board, and IMU connection board. The main control board, equipped with an ultra-low-power microcontroller, serves as the system’s core, offering circuit protection, power management, and Bluetooth transmission. To minimize discomfort, the flex sensor connection board is designed in an "L" shape with dual-sided solder pads secured with adhesive to increase durability, while the IMU connection board has a rounded square shape with the solder pads placed on the back.

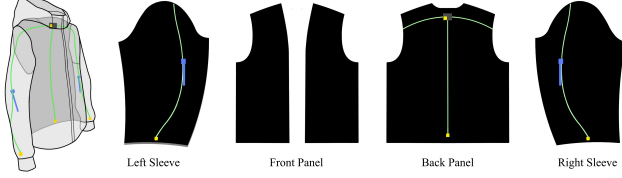


Figure 4: Garment pattern design and sensor placement of our prototype. Blue: Flex Sensor; Yellow: IMU; Green: Wire.

Garment Design. The design of the garment patterns for our prototype, including the placement of sensors on these patterns, is illustrated in Fig. 4. Through this pattern design, we defined the shapes of the fabric pieces required for garment construction. During the prototyping process, we will use this design to mark the placement of the sensors to ensure accurate integration.

3.2 Prototyping

The prototype production consists of three stages: sensor assembly, fabric cutting, and garment integration (Fig. 5).

Sensor Assembly. First, the flex sensors and IMUs are soldered onto their respective connection boards. The main control board is then connected to the two flex sensors and four IMUs via two I^2C buses and four UART channels, completing the sensor assembly.

Fabric Cutting. Based on garment design, full-scale paper garment patterns are printed. These patterns are placed directly on the nylon fabric surface. The fabric is then cut according to these patterns, and the wiring and sensor placement are marked on the cut fabric pieces.

Garment Integration. The assembled sensors are integrated into the garment through heat pressing. First, the heat adhesive film is cut and heat-pressed onto the fabric. Next, the lining is sewn, and the adhesive film is bonded to the fabric to create wiring channels. Finally, the outer fabric is sewn to the lining, completing the double-layered smart garment.

4 FIP for Sensor Displacements

To address the sensor displacements in loose-fitting garments, FIP integrates three key components: 1) a Displacement Latent Diffusion Model (DLDM) for generating sufficient IMU *Real-time Displacement* data to train a robust motion estimation model; 2) a Physics-informed Calibrator (PIC) to register flex sensor data in different *Primary Displacements*; 3) a Pose Fusion Predictor (PFP) to fuse multi-modal sensor readings with elbow joint focus.

Fig. 6 illustrates the overview of our pipeline. Overall, our objective is to estimate human body posture using readings from flex sensors and IMUs integrated into a loose-fitting daily garment. The input to our model includes measurements from 4 IMUs ($\text{IMU} \in \mathbb{R}^{4 \times 9}$) and 2 flex sensors ($\text{Flex} \in \mathbb{R}^{2 \times 1}$). The output of the model is the upper body postures represented by the 3D rotation angles of 10 joints ($\theta \in \mathbb{R}^{10 \times 3}$).

Training Phase. Firstly, as capturing IMU *Real-time Displacement* in the real world is very challenging, we utilize a simulation fabric-body model to synthesize displacement data, denoted as IMU_{sim} . Then, for training a robust pose predictor, we train a Displacement Latent Diffusion Model (DLDM) to generate enough diverse data that covers real-world distribution. In addition, we simulate the flex sensor readings Flex_{sim} by calculating the angle between the forearm and upper arm skeleton. Flex sensor data Flex_{sim} and generated IMU data $\text{DLDM}(\text{IMU}_{sim})$ will be input to train a Pose Fusion Predictor (PFP), with the supervision from simulated SMPL Pose. The training phase can be denoted as:

$$\theta = \text{PFP}(\text{DLDM}(\text{IMU}_{sim}), \text{Flex}_{sim}) \quad (4)$$

Testing Phase. Physical-informed Calibrator (PIC) is only employed in the real-world testing phase, to correct the flex sensor readings into real motion ranges. Then, the flex and IMU sensor readings IMU and calibrated Flex will input to PFP for the estimation of pose θ , denoted as:

$$\theta = \text{PFP}(\text{IMU}, \text{PIC}(\text{Flex})) \quad (5)$$

4.1 Inertial Sensors: Displacement Latent Diffusion Model

Challenge: *Real-time displacement occurs as sensors shift and vibrate due to loose-fitting clothing. However, developing a machine learning model for real-time displacement presents significant challenges: 1) capturing real-time displacement data in real-world scenarios is highly difficult, and 2) the variability in user poses, body shapes, clothing fits, and random movements introduces substantial randomness, complicating the accurate simulation of real-time displacement.*

Fig. 7 illustrates the overview our Displacement Latent Diffusion Model (DLDM). Our approach leverages the powerful capabilities of deep generative models to learn a representative latent space of IMU displacement z from displacement x_{dis} . From this latent space z , we can generate diverse and realistic IMU displacement signals x_{dis}^{gen} , enabling the training of a robust pose estimation model. To achieve this, we first establish a simulation framework to retrieve simulated IMU displacement data x_{dis} . Then, we train the DLDM via a dual-stage process that hierarchically optimizes x_{dis} into a standard Gaussian distribution z . In the first stage, we train the model as a regular Variational Autoencoder (VAE) [25] with standard Gaussian priors. Subsequently, we refine the latent encodings by training the latent Denoising Diffusion Models (DDMs) [17].

4.1.1 Displacement Simulation. As collecting the IMU displacement data in the real world is very challenging, we propose a simulation framework to obtain IMU *Realtime Displacement* data. Firstly, we simulate tight-wearing IMU signals by directly placing the virtual IMUs on the human body mesh obtained from the

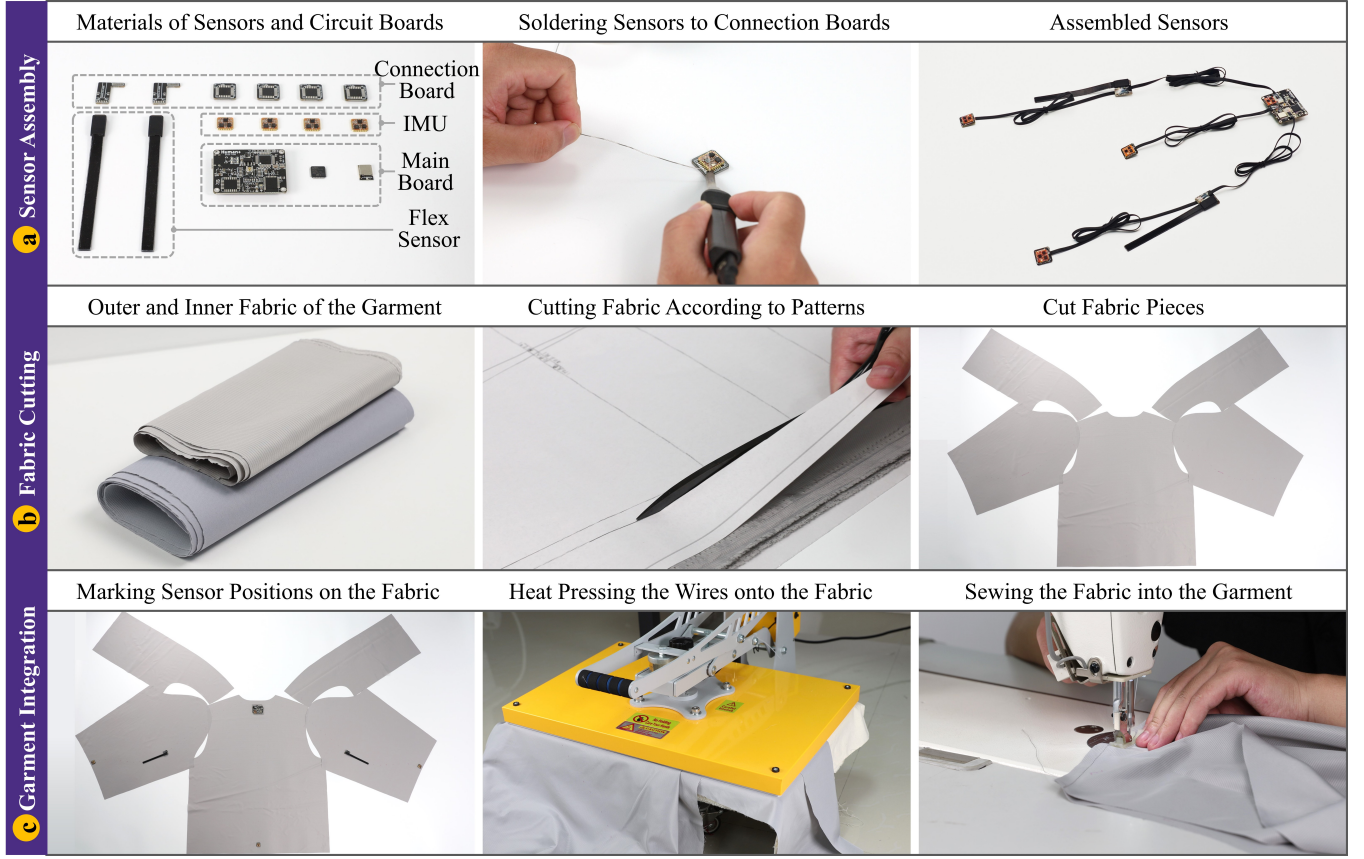


Figure 5: The process of prototyping: (a) Assemble the sensors together by soldering; (b) Cut the fabric into pieces according to the patterns; (c) Integrate the assembled sensors into the fabric through heat pressing and sew the fabric into the garment.

AMASS dataset [39], and then utilize TailorNet [51] to simulate topologically consistent clothing given SMPL pose and body shape to obtain loose IMU data as described in [88]. Finally, we subtract the simulation IMU in the loose garment and tight-wearing IMU data to obtain the real-time displacement x_{dis} .

4.1.2 First Stage Training. In the first stage of training, FIP is trained by optimizing the encoder and decoder parameters ϕ and ξ to learn an expressive IMU displacement latent z_0 by minimizing:

$$\mathcal{L}(\xi, \phi; x_{dis}) = \mathbb{E}_{q_\phi(z_0|x_{dis})} [\log p_\xi(x|z_0)] - \lambda_{KL} D_{KL}(q_\phi(z_0|x) \parallel p(z_0)), \quad (6)$$

Here, the IMU displacement latent z_0 is sampled from the encoded posterior distribution $q_\phi(z_0|x_{dis})$, whose means and variances are predicted via VAE’s encoder. Furthermore, $p_\xi(x|z_0)$ denotes the decoder, parametrized as a Laplace distribution with predicted means and fixed unit scale parameter. λ_{KL} are hyperparameters balancing reconstruction accuracy and Kullback-Leibler regularization.

4.1.3 Second Stage Training. In principle, we could use the VAE’s priors to sample encodings and generate various displacements. However, we find that simple displacement latent from VAE does not accurately match the real-world displacement distribution from

the training data, leading to poor samples (*i.e.*, the prior hole problem) [64]. This limitation motivates the use of highly expressive latent diffusion models (LDMs). Specifically, in the second stage, we freeze the VAE’s encoder and decoder networks and add Gaussian noise on the encodings z_0 sampled from $q_\phi(z_0|x)$ gradually until z_0 becomes normal gaussian distribution $p(z_T) \sim \mathcal{N}(0, I)$. Then, we could train a denoising diffusion model θ to reverse the diffusion process, which translates the latent $p(z_T)$ back to the original IMU displacement latent space.

4.1.4 Generation. With the expressive LDMs, we can formally define a hierarchical generative model $p_{\xi, \theta}(x, z_0) = p_\xi(x|z_0)p_\theta(z_0)$ denotes the distribution of the displacement latent, and $p_\xi(x|z_0)$ is FIP’s Decoder. We can hierarchically sample from latent and generate diverse IMU displacements x_{dis}^{gen} with the VAE decoder.

With the generated diverse IMU displacements data x_{dis}^{gen} , we could train our robust pose estimation model, Pose Fusion Predictor. We will discuss the data and model architecture of VAE and LDMs in detail in Sec. 5.

4.2 Flex Sensors: Physics-informed Calibrator

Challenge: Primary displacement during clothing donning alters sensor placement due to significant body-clothing contact, causing

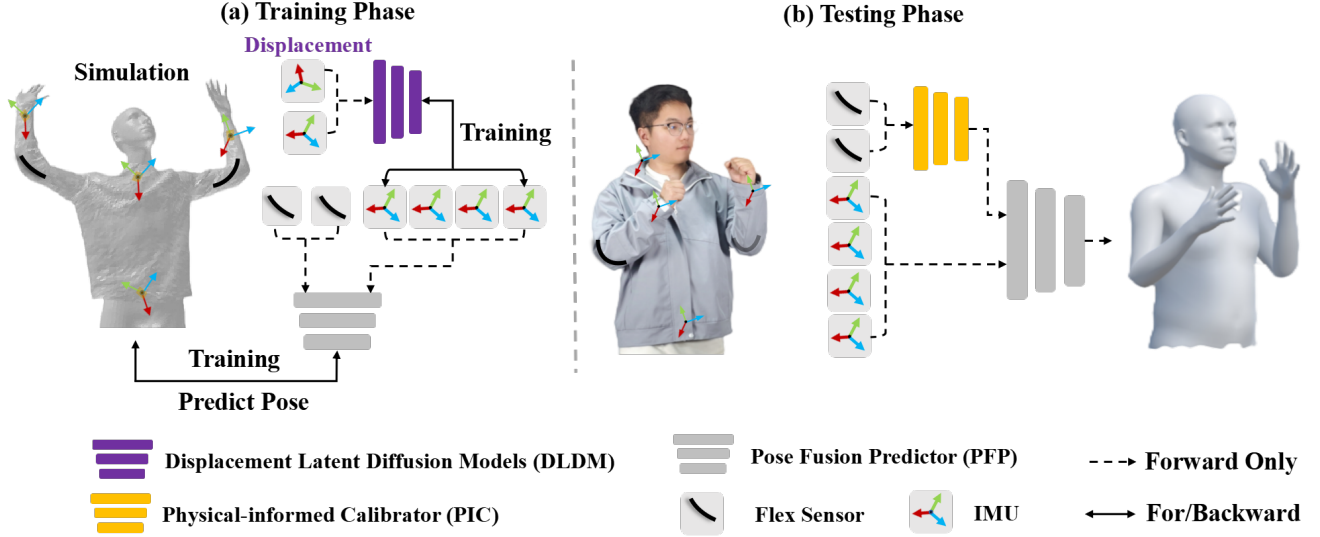


Figure 6: Pipeline Overview. Left: For data preparation, we first utilize a simulation body-fabric model to synthesize the IMU *Real-time Displacement*. Then, for training a robust pose predictor, we train a Displacement Latent Diffusion Model (DLDM) to generate enough diverse data that covers real-world distribution. At last, we train a Pose Fusion Predictor leveraging simulated flex sensor data and generated IMU data, with the supervision of SMPL Pose [32]. Right: In our testing phase, flex sensor readings will be firstly input to our Physical-informed Calibrator to address the *Primary Displacement*, which will be input to the pre-trained Pose Fusion Predictor with IMU data.

substantial data distribution discrepancies. This challenges models trained on synthetic displacement data to capture real-world displacement features. Hence, efficient calibration of *Primary Displacement* is crucial for accurate measurements with flex sensors.

To address this, we introduce a Physics-informed Calibrator (PIC), which calibrates *Primary Displacement* through a single elbow flexion. The PIC module is designed and implemented based on our observation that, despite significant shifts in sensor data range due to *Primary Displacement*, the displaced sensor data are always aligned with the overall movement patterns. Therefore, by performing a full vertical elbow bend, we can recalibrate the sensor data to match the actual motion angles by realigning the data range, ensuring the measurements remain physically accurate. In general, our PIC module can be written as:

$$\theta^C = PIC(\theta) = \frac{\theta - \theta_{min}}{\theta_{max} - \theta_{min}} \times (\theta_{max}^C - \theta_{min}^C) + \theta_{min}^C \quad (7)$$

which θ^C represents the sensor readings after PIC, and the minimum and maximum range for calibrating data are denoted as θ_{min}^C and θ_{max}^C . In our setup, the user performs a full vertical elbow bend, so we define $\theta_{min}^C = 0$ and $\theta_{max}^C = 90$. Similarly, θ^{raw} refers to the raw sensor data, and its minimum and maximum range θ_{min} , and θ_{max} is collected in our calibration process, respectively. According to the Eq. 7, we could scale the raw sensor data $\theta \in (\theta_{min}, \theta_{max})$ to the corrected motion angle data $\theta^C \in (\theta_{min}^C, \theta_{max}^C)$, ensuring physical accuracy.

$$\frac{\theta^C - \theta_{min}^C}{\theta_{max}^C - \theta_{min}^C} = \frac{\theta - \theta_{min}}{\theta_{max} - \theta_{min}} \quad (8)$$

4.3 Pose Fusion Predictor (PFP)

The structure of the Pose Fusion Predictor is depicted in Fig. 9. The goal of the PFP is to estimate the 3D joint rotations $\theta \in \mathbb{R}^{10 \times 3}$ using the flex and inertial sensor readings **Flex** and **IMU**. It is composed of 3 long short-term memory (LSTM) layers.

Firstly, the Position LSTM utilizes four Inertial sensor readings **IMU** to predict joint positions $p \in \mathbb{R}^{11 \times 3}$. Then we decompose our θ prediction into two stages. The first Rotation LSTM combines **Flex**, **IMU**, and p to predict the two elbow joint rotations $\theta_e \in \mathbb{R}^{2 \times 3}$, whereas another Rotation LSTM combines p and **IMU** to predict other joint rotations $\theta_o \in \mathbb{R}^{8 \times 3}$. θ_e is then concatenated with θ_o to form the final joint rotation output θ .

To improve the predictions of elbow joints, which obtain a large degree of freedom and movement range, we include an additional Elbow Focus Loss \mathcal{L}_E . This loss encourages the attention to the elbow joint by computing the elbow bending angle through forward kinematics when training the first Rotation LSTM.

To train our PFP, the total loss \mathcal{L} is defined as a weighted sum of three components: \mathcal{L}_p corresponds to the prediction of joint positions p ; \mathcal{L}_θ corresponds to the prediction of joint rotations θ ; \mathcal{L}_E ensures the model pays special attention to accurate elbow rotation prediction. All losses are Mean Squared Error (MSE) between ground truth and prediction. The full loss function can be expressed as:

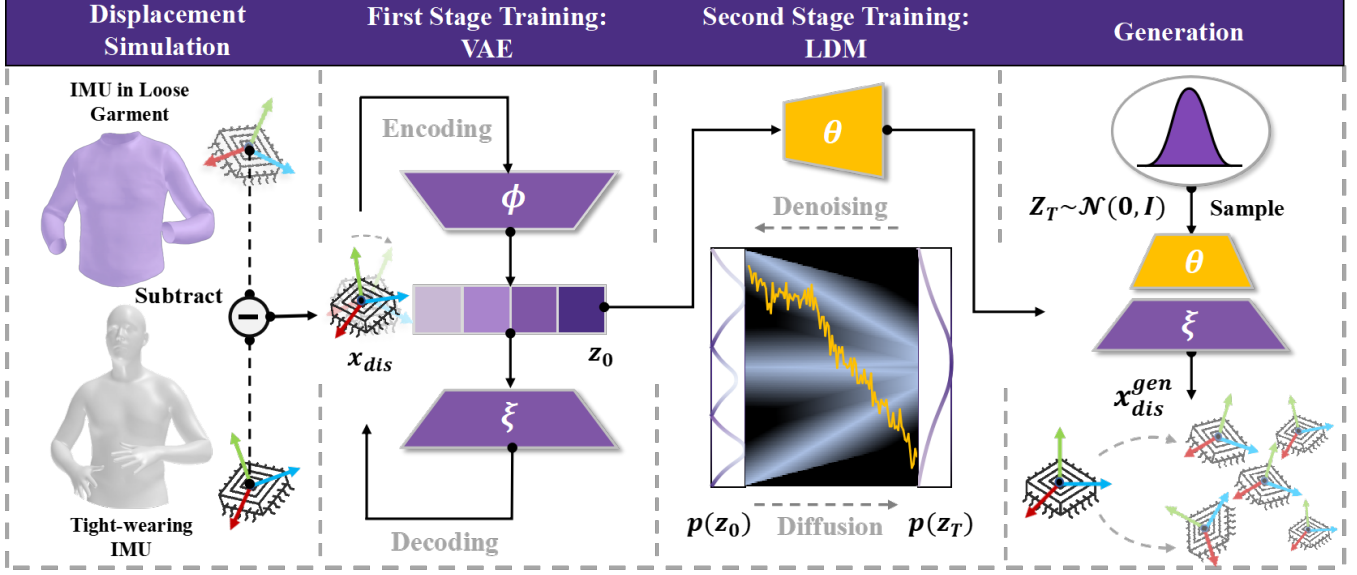


Figure 7: Overview of Displacement Latent Diffusion Model (DLDM). (a) Firstly, the *Real-time Displacement* x_{dis} could be captured through subtracting paired Loose and Tight IMU simulation data; (b) After obtaining displacement x_{dis} , we trained a Variational Autoencoder (VAE) to encode an expressive displacement latent z_0 with respect to the encoder and decoder parameters ϕ and ξ ; (c) Then, we freeze the VAE’s encoder and decoder networks and train Latent Diffusion Models (LDM) on the sampled latent z_0 , which gradually become normal gaussian distribution $z_T \sim \mathcal{N}(0, I)$ through noise diffusion process. (d) Finally, with the expressive LDMs, we can define a hierarchical generative model to generate various displacements x_{dis}^{gen} with LDM’s denoising network θ and VAE’s Decoder ξ from Gaussian noise z_T .

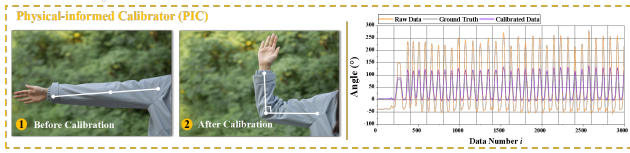


Figure 8: The process and effect of Physics-informed Calibrator. Through one elbow flexion calibration, our PIC could rectify flex sensors readings effectively.

$$\mathcal{L} = \lambda_1 \mathcal{L}_p + \lambda_2 \mathcal{L}_\theta + \lambda_3 \mathcal{L}_E \quad (9)$$

where $\lambda_1, \lambda_2, \lambda_3$ are the weighting factors that control the influence of each component. By minimizing this total loss, our PFP is trained to enhance overall pose estimation accuracy, with a particular focus on elbow prediction.

5 Experiments

In this section, we first describe the dataset, metrics, and training details used in our approach (Sec. 5.1). We then present the results of our method compared to SOTA real-time posture estimation methods (Sec. 5.2), followed by an ablation study to analyze the impact of proposed techniques (Sec. 5.3). Finally, we demonstrate the real-time motion capture interface of our approach (Sec. 5.4).

5.1 Implementation

5.1.1 Dataset. Our dataset consists of two parts: the Simulation Dataset D_{sim} , D_{sim}^{dis} and the Real Dataset D_{real} . The D_{sim} and D_{sim}^{dis} are employed for training our models, whereas the real data D_{real} is utilized for testing purposes.

- D_{sim} : We simulated tight-wearing IMU signals by directly placing the virtual IMUs on the human body mesh obtained from the AMASS dataset [39], using the method described above. Notably, we adapted the joint and mesh vertex settings to match our upper body IMU setup (left forearm, right forearm, back, and waist).
- D_{sim}^{dis} : Collecting the IMU displacement data in the real world is challenging as we could not directly capture the paired real-time tight-wearing and loose-wearing IMU data. Hence, we firstly followed the methodology developed for loose IMU sensors based on D_{sim} as described in LIP [88], which utilized TailorNet to simulate topologically consistent clothing given SMPL pose and body shape. Then, we subtracted the simulation loose IMU data and the aforementioned tight-wearing IMU data to obtain the real-time disturbance.
- D_{real} : We recruited a total of ten individuals with varying body shapes and collected a real-world dataset for evaluation using our flex-and-IMU fusion garment. All participants were informed of the experiment’s purpose and signed the consent agreement for participation. During data collection, participants were asked to perform ten predefined actions,

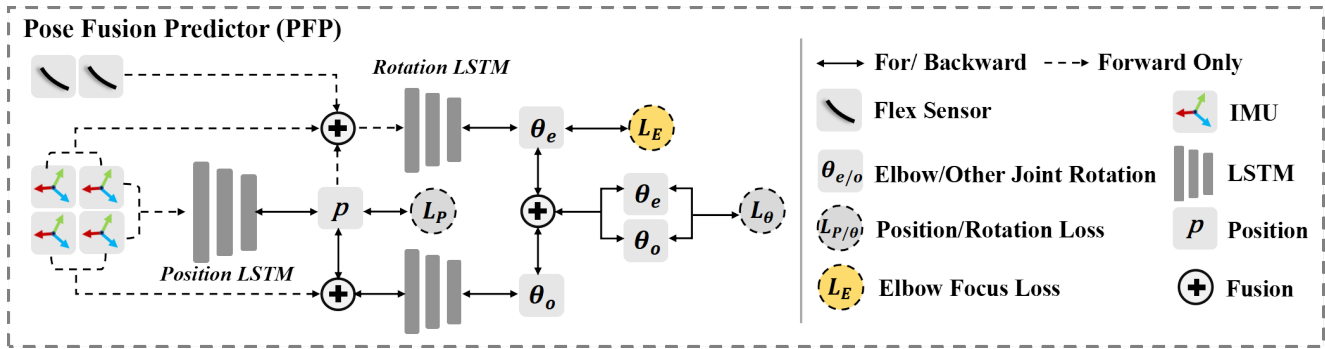


Figure 9: Structure of Pose Fusion Predictor. First, the Position LSTM uses four IMU readings to predict joint positions $p \in \mathbb{R}^{11 \times 3}$. The rotation prediction is then split into two stages. One Rotation LSTM combines Flex, IMU, and p to predict elbow joint rotations $\theta_e \in \mathbb{R}^{2 \times 3}$, while the other combines p and IMU to predict the remaining joint rotations $\theta_o \in \mathbb{R}^{8 \times 3}$. Finally, θ_e and θ_o are concatenated to produce the full joint rotation output θ . PFP is trained by Position Loss L_p and Rotation Loss L_θ , with an additional Elbow Focus Loss L_E to improve the predictions of elbow joints.

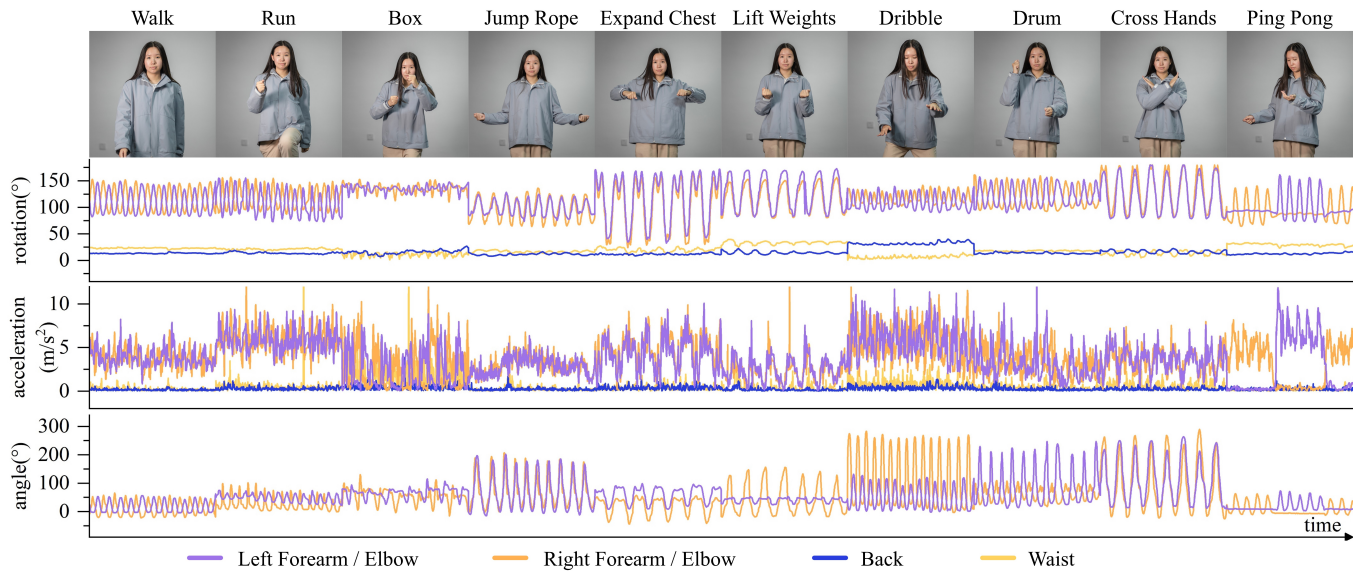


Figure 10: Flex sensor and IMU signals. We present the sensor readings from both the flex sensors and IMUs while the user performs various actions, including walking, running, boxing, jumping rope, expanding the chest, lifting weights, dribbling, drumming, crossing hands, and playing ping pong.

including walking, running, boxing, and more. Each action lasted for one minute. We present the sensor readings while the user performs various actions in Fig. 10. For the ground truth pose, we used the Perception Neuron 3 system³ to capture upper-body poses using 11 tight-wear IMUs. Overall, we collected 371,122 frames of 60 fps data, with a total duration of about 2 hours. More information can be found in the supplementary materials.

5.1.2 *Evaluation Metrics.* Following TransPose [76], we measure the accuracy of pose estimation using the following four metrics:

- Angular Error ($^\circ$), which measures the mean rotation error of ten upper body joints in degrees;
- Positional Error (cm), which measures the mean Euclidean distance error of 12 upper body joint endpoints in centimeters. Note that in practice, we only calculate the positional error of eleven joint endpoints as the position of the pelvis joint is kept at $[0, 0, 0]$.
- Elbow Angular Error ($^\circ$), which measures the mean rotation error of two elbow joints in degrees.
- Jitter (m/s^3), which measures the average jerk of 12 upper body joints.

³<https://neuronmocap.com/pages/perception-neuron-3/>

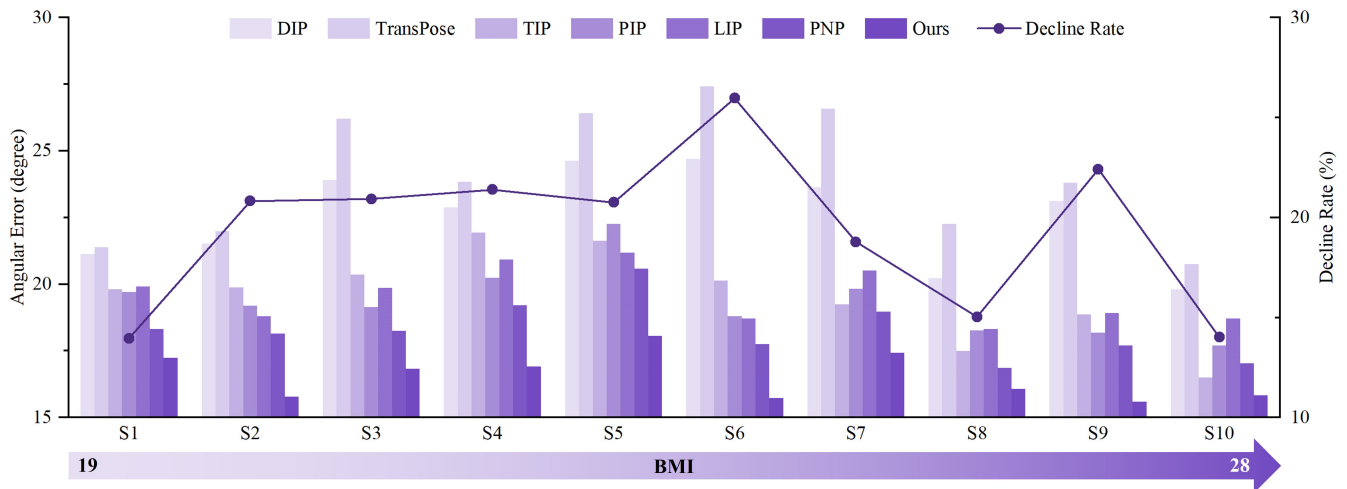


Figure 11: Experimental results of Angular Error (unit: degree) on ten participants. The S1 indicates the subject with ID=1. The Decline Rate reflects the rate at which the error decreases in FIP.

5.1.3 Training Details. All our experiments run on a computer with an Intel(R) Core(TM) i7-13700K CPU and an NVIDIA RTX 4080 GPU. The model is implemented using PyTorch 2.4.0 with CUDA 11.8. Please refer to the supplementary material for the training details and PFP network structure.

- Training the Displacement Latent Diffusion Model. VAE and Diffusion Models were both trained with D_{sim}^{dis} , utilizing a batch size of 512. We set $\lambda_{KL} = 1e^{-8}$ to prevent over-regularization and enhance the fidelity of the generated results. The Adam optimizer was used with a learning rate of $lr = 1e^{-3}$ during training.
- Training Pose Fusion Predictor. The pose estimation network was trained with D_{sim}^{dis} and D_{sim} , utilizing a batch size of 512. We set $\lambda_1 = 4$, $\lambda_2 = 1$, and $\lambda_3 = 0.1$. The Adam optimizer was used with a learning rate of $lr = 5e^{-4}$ and weight decay = $1e^{-5}$ during training.

5.2 Results

Our model predicts upper body poses with an angular error of 16.54° (a 19.5 % improvement), an elbow angular error of 25.27° (a 26.4 % improvement), and a position error of 8.06 cm (a 30.1 % improvement) compared with SOTA real-time *Inertial-based MoCap* methods, including DIP [19], TransPose [76], TIP [21], PIP [75], LIP [88], and PNP [77]. Since most of these SOTA methods are designed for tight-wear IMUs with different sensor numbers and installation positions, we followed the official code provided by the authors and retrained the models using D_{sim} and reported the angular and positional errors on D_{real} . For LIP, we adopted the released model without any change.

As illustrated in Fig. 11 to 13 and Tab. 2, our method surpasses all SOTA motion capture techniques, including those using tight-wearing IMU methods (e.g., PIP, PNP) and previous clothing-based IMU approaches (e.g., LIP). This demonstrates a significant advantage in robustness across a diverse range of body shapes and motions.

Notably, as shown in Fig. 12 and Fig. 14, our method can substantially reduce the elbow angular error, which is crucial for various real-world applications. This underscores the benefits of integrating IMUs with sensors in our approach.

5.3 Ablation Study

We evaluate the effectiveness of the proposed Displacement Latent Diffusion Model, Physical-informed Calibrator, and Pose Fusion Predictor in Fig. 15. The results demonstrate that all three proposed techniques are necessary to achieve the best performance.

Additionally, since our synthesis of IMU *Real-time Displacement* is fundamentally a conditional generation task, we compared our DLDM generator with the generator of LIP and evaluated the effectiveness of Diffusion in DLDM. We assessed the richness and quality of the generated IMU displacement data quality using metrics such as FID, PSNR, and SSIM [58], as detailed in Tab. 3. Besides, the generated IMU displacement data were compared using t-SNE dimensionality reduction, as illustrated in Fig. 16. These evaluations demonstrate the significance of Diffusion in DLDM and highlight the superiority of DLDM over LIP. The IMU displacement data generated by our DLDM offers better fidelity and diversity compared to LIP. This enhancement enables our approach to more effectively simulate real-time IMU displacements in practical applications.

5.4 Real-time MoCap

We implemented a real-time MoCap visualization interface using Python and Unity (Fig. 17). When the user dons our garment as common, the system initiates with a T-pose calibration (5 seconds) followed by an elbow flexion calibration (1 second). During operation, the system continuously receives real-time IMU and flex sensor readings. The IMU readings are calibrated and normalized using methods similar to those in TransPose[76], while the flex sensor readings are calibrated separately through the PIC. Both readings are then input into the PFP to achieve real-time motion capture outputs. Through the real-time MoCap visualization, we

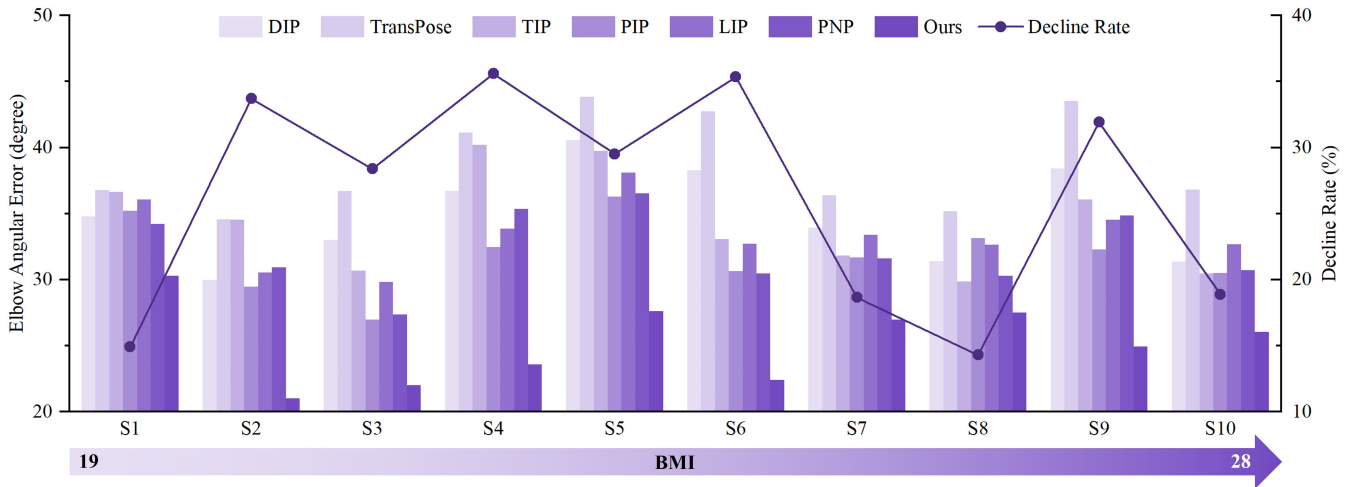


Figure 12: Experimental results of Elbow Angular Error (unit: degree) on ten participants. The S1 indicates the subject with ID=1. The Decline Rate reflects the rate at which the error decreases in FIP.

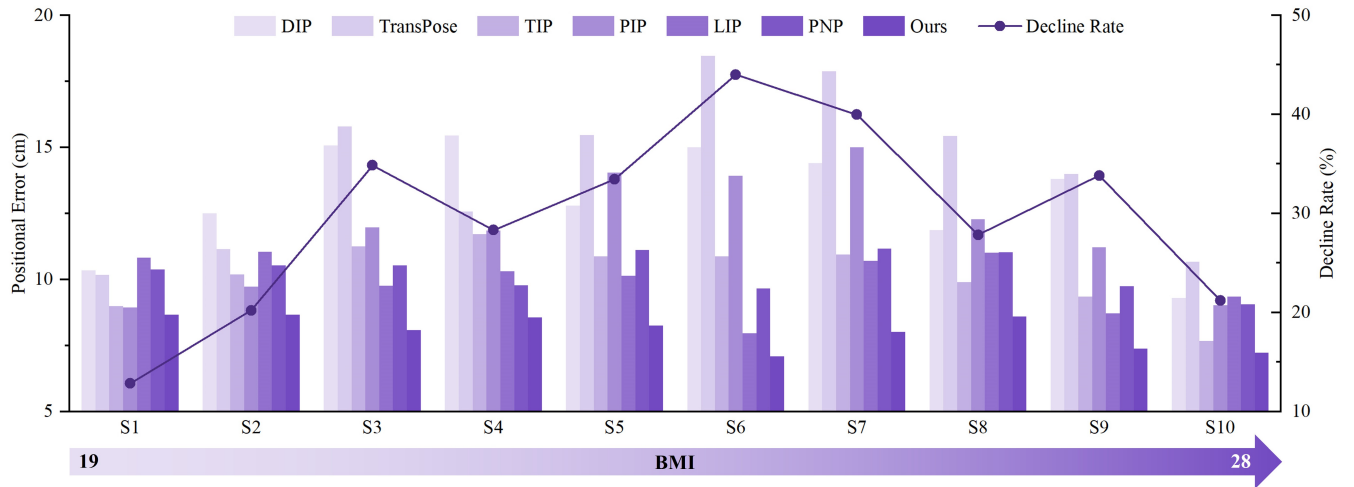


Figure 13: Experimental results of Positional Error (unit: cm) on ten participants. The S1 indicates the subject with ID=1. The Decline Rate reflects the rate at which the error decreases in FIP.

Table 2: Comparison with SOTA real-time *Inertial-based MoCap* methods. Our approach significantly reduces elbow tracking errors and achieves SOTA performance in overall joint motion capture, surpassing all competing approaches.

System	Angular Error (°)	Elbow Angular Error (°)	Position Error (cm)	Jitter (m/s ³)
DIP	22.53 ± 5.26	34.90 ± 13.25	13.02 ± 5.17	0.34
TransPose	23.98 ± 5.57	38.84 ± 12.11	14.03 ± 6.05	0.13
TIP	19.61 ± 6.29	34.49 ± 14.00	10.16 ± 4.60	2.00
PIP	19.29 ± 6.04	31.95 ± 15.77	11.72 ± 5.27	0.37
LIP	19.58 ± 5.03	33.50 ± 12.48	9.99 ± 4.19	0.17
PNP	18.29 ± 4.17	32.37 ± 12.44	10.29 ± 2.91	0.36
Ours	16.54 ± 3.76	25.27 ± 11.15	8.06 ± 2.87	0.05

demonstrate the system’s convenience, comfort, and robustness in

motion capture, particularly excelling in elbow movement tracking.

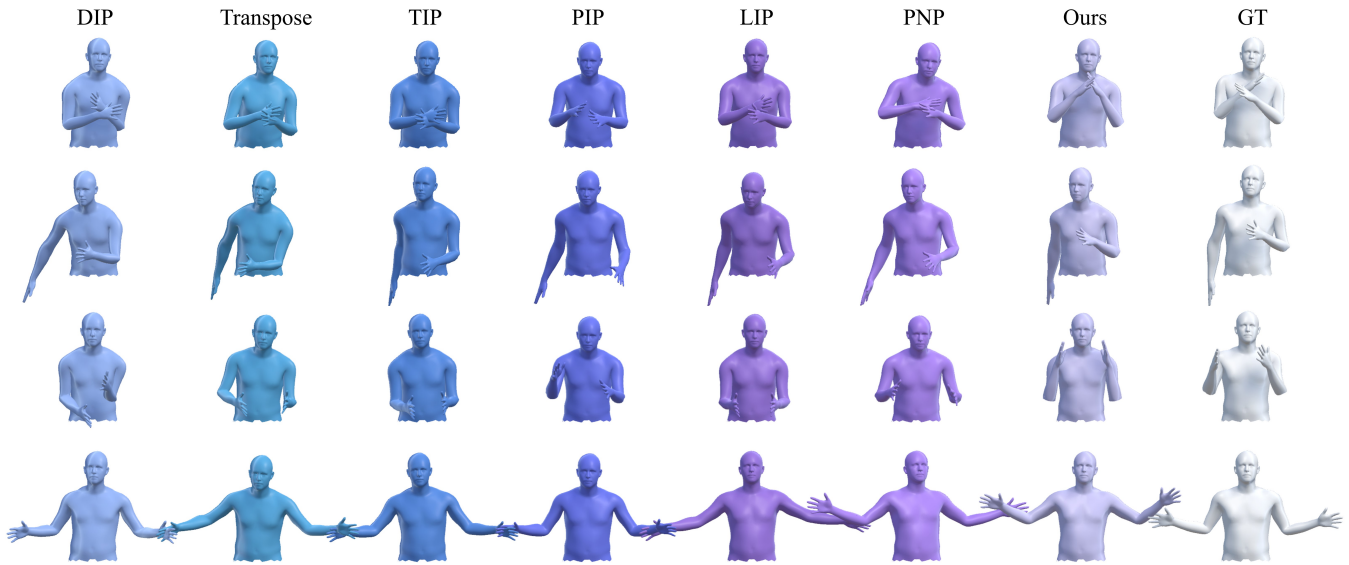


Figure 14: Qualitative results: our approach outperforms all SOTA methods in motion capture with a clear advantage in elbow joint tracking.

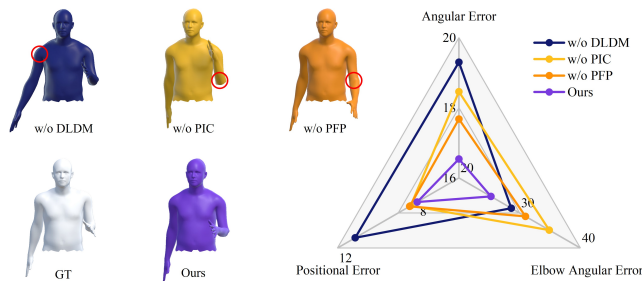


Figure 15: The results of the ablation study show that the performance declines when any component of DLDM, PIC, or PFP is removed, indicating that all three components are essential.

Table 3: Quantitative results of ablation study of DLDM. These results demonstrate the significance of Diffusion in DLDM and highlight the superiority of DLDM over LIP.

Method	FID↓	PSNR↑	SSIM↑
LIP	1.54	11.26	0.73
DLDM (w/o Diffusion)	1.48	10.26	0.70
DLDM (Ours)	1.17	12.51	0.78

A demonstration video of the real-time MoCap system is provided in the supplementary materials.

6 Applications

We demonstrate applications of our *Clothes-based MoCap* system in various human-computer interaction scenarios, including virtual

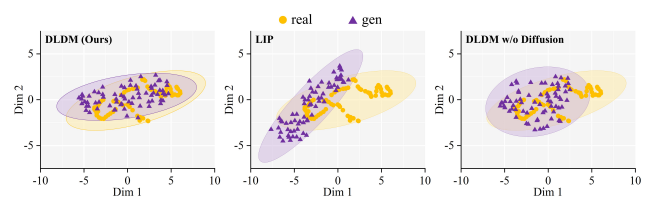


Figure 16: Qualitative results of ablation study of DLDM. We use t-SNE to visualize IMU displacement generated by DLDM, LIP, and DLDM without Diffusion, respectively. The image shows: i) our DLDM generates more realistic IMU displacement data than LIP; ii) removing the proposed Diffusion Model will degrade the similarity with real-world data, highlighting the significance of Diffusion in DLDM.

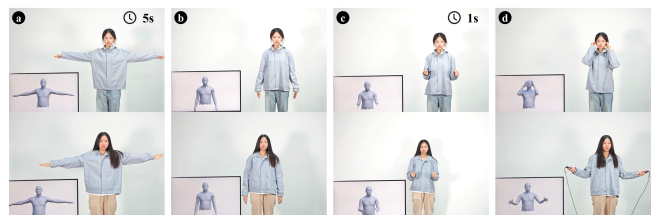


Figure 17: Demonstration of the real-time MoCap visualization system. (a) a T-pose calibration (5 seconds); (b-c) an elbow flexion calibration (1 second); (d) real-time MoCap visualization result.

and augmented reality (VR/AR), rehabilitation, and fitness analysis (Fig. 18), leveraging the system's robustness, accessibility, and comfort.



Figure 18: Applications of our approach: (a) Metaverse, (b) rehabilitation, (c) fitness analysis.

6.1 Virtual & Augmented Reality

MoCap is essential for AR/VR, facilitating the creation of digital twins in the Metaverse and providing a realistic experience for users. Our garment-based system offers superior privacy protection compared to visual capture solutions, mitigating risks of information leakage associated with cameras. It also serves as a self-contained system, eliminating the need for external cameras and remaining unaffected by visual occlusion. Additionally, unlike other wearable devices that often require tight-fitting, our loose-fitting system ensures ease of use and comfort while maintaining accurate and reliable motion capture. This allows users to effectively control their avatars in the virtual world (Fig. 18a), unlocking new possibilities for immersive interaction in AR/VR applications.

6.2 Rehabilitation

Home rehabilitation has a significant need for ubiquitous and longitudinal monitoring. Our garment-based system is particularly well-suited for home rehabilitation monitoring because of its robustness, comfort, and seamless integration. Unlike conventional medical devices, the garment is a non-intrusive and lifestyle-friendly solution that patients can wear as regular garments continuously in everyday life. Through our system, healthcare providers can remotely and in real-time monitor patient progress and offer personalized treatment recommendations based on captured motion data (Fig. 18b). This approach not only improves patient adherence during rehabilitation but also enhances comfort and privacy.

6.3 Fitness Analysis

In the domain of fitness and sports, MoCap is widely used to analyze techniques, prevent injuries, enhance performance, and tailor personalized training programs by providing detailed insights into movement patterns and biomechanics. Our *Clothes-based MoCap* method provides an effective and practical approach for motion capturing in both indoor and outdoor activities, eliminating the need for complex setups or additional equipment. By collecting and analyzing motion data in real-time, the system can effectively assess user posture and activity levels, offering tailored exercise recommendations (Fig. 18c). The combination of flex sensors and IMUs ensures reliable motion capture, aiding users in adjusting their training regimens for optimal results.

7 Discussion

7.1 Clothes-based MoCap

Advantages. Clothing provides an efficient medium for sensor fusion, which can significantly enhance motion capture accuracy without compromising user comfort. As a compelling exploration, FIP leverages both IMUs and flexible bend sensors, capitalizing on the strengths of each to improve motion capture precision, particularly in accurately measuring elbow joint angles. This approach could inspire researchers to incorporate a wide range of sensors, such as ToF, laser, radar, and ultrasound. More importantly, we emphasize that this fusion has the potential to revolutionize the limitations of previous sensor measurement paradigms, enabling biomechanical functions beyond simple joint tracking. For instance, some studies have utilized flexible strain sensors to measure the wearer’s body dimensions, which, when integrated with IMUs, could allow for the simultaneous capture of both body shape and motion. Consequently, Clothes-based motion capture through sensor fusion holds significant promise for applications in fitness analysis, rehabilitation, and more.

Disadvantages. While integrating multiple sensors into clothing can significantly enhance motion capture accuracy, it also increases manufacturing complexity and costs. Additionally, the need to develop algorithms to address the unique displacement issues of each sensor presents further challenges in algorithm design.

7.2 Limitations & Future works

On the hardware side, although we have conducted comparisons with different users, the impact of clothing sizes and fabric materials on accuracy remains to be explored. *On the software side,* although we have addressed the *Primary Displacement* of flex sensors when users first don the clothing, as the *Real-time Displacement* of the flex sensors located at the elbow is minimal in our garment. However, real-time correction of significant sensor displacements that may occur later (e.g., due to forceful tugging during movement) remains an open challenge. In the future, we plan to explore solutions to this issue to further enhance accuracy.

8 Conclusion

In this paper, we introduced Flexible Inertial Poser (FIP), a novel approach for achieving real-time, accurate pose estimation through the fusion of flex and inertial sensors. Our key innovation lies in the hardware prototype and software design of the sensor fusion garment. Specifically, FIP introduces a Displacement Latent Diffusion Model to synthesize sensor disturbance in various conditions from limited simulation data, as well as a Physics-informed Calibrator to rectify the *Primary Displacement* of flex sensors. Extensive experiments demonstrate that our method achieves robust performance across varying body shapes and motions, significantly outperforming SOTA approaches with a 19.5% improvement in angular error, a 26.4% improvement in elbow angular error, and a 30.1% improvement in position error. As the first endeavor to integrate flex and inertial sensors in a MoCap garment, our work aims to inspire advancements in *Clothes-based MoCap* within the HCI community.

References

- [1] Thiemo Alldieck, Marcus Magnor, Weipeng Xu, Christian Theobalt, and Gerard Pons-Moll. 2018. Video based reconstruction of 3d people models. In *Proceedings of the IEEE Conference on Computer Vision and Pattern Recognition*. 8387–8397.
- [2] Oresti Baños, Miguel Damas, Héctor Pomares, Ignacio Rojas, Máté Attila Tóth, and Oliver Amft. 2012. A benchmark dataset to evaluate sensor displacement in activity recognition. In *Proceedings of the 2012 ACM Conference on Ubiquitous Computing*. 1026–1035.
- [3] Oresti Banos, Mate Attila Toth, Miguel Damas, Hector Pomares, and Ignacio Rojas. 2014. Dealing with the effects of sensor displacement in wearable activity recognition. *Sensors* 14, 6 (2014), 9995–10023.
- [4] Jeroen HM Bergmann, Salzitsa Anastasova-Ivanova, Irina Spulber, Vivek Gulati, Pantelis Georgiou, and Alison McGregor. 2013. An attachable clothing sensor system for measuring knee joint angles. *IEEE Sensors Journal* 13, 10 (2013), 4090–4097.
- [5] Hanqun Cao, Cheng Tan, Zhangyang Gao, Yilun Xu, Guangyong Chen, Pheng-Ann Heng, and Stan Z Li. 2024. A survey on generative diffusion models. *IEEE Transactions on Knowledge and Data Engineering* (2024).
- [6] Youngjae Chang, Akhil Mathur, Anton Isopoussu, Junehwa Song, and Fahim Kawsar. 2020. A systematic study of unsupervised domain adaptation for robust human-activity recognition. *Proceedings of the ACM on Interactive, Mobile, Wearable and Ubiquitous Technologies* 4, 1 (2020), 1–30.
- [7] Anargyros Chatzitofis, Dimitrios Zarpalas, Petros Daras, and Stefanos Kollias. 2021. DeMoCap: Low-cost marker-based motion capture. *International Journal of Computer Vision* 129, 12 (2021), 3338–3366.
- [8] Xiaowei Chen, Xiao Jiang, Jiawei Fang, Shihui Guo, Juncong Lin, Minghong Liao, Guoliang Luo, and Hongbo Fu. 2023. DisPad: Flexible On-Body Displacement of Fabric Sensors for Robust Joint-Motion Tracking. *arXiv preprint arXiv:2301.06249* (2023).
- [9] Xiaowei Chen, Xiao Jiang, Lishuang Zhan, Shihui Guo, Qunsheng Ruan, Guoliang Luo, Minghong Liao, and Yipeng Qin. 2023. Full-body human motion reconstruction with sparse joint tracking using flexible sensors. *ACM Transactions on Multimedia Computing, Communications and Applications* 20, 2 (2023), 1–19.
- [10] Rohan Choudhury, Kris M Kitani, and László A Jeni. 2023. TEMPO: Efficient multi-view pose estimation, tracking, and forecasting. In *Proceedings of the IEEE/CVF International Conference on Computer Vision*. 14750–14760.
- [11] Shohreh Deldari, Hao Xue, Aaqib Saeed, Daniel V Smith, and Flora D Salim. 2022. Cocoa: Cross modality contrastive learning for sensor data. *Proceedings of the ACM on Interactive, Mobile, Wearable and Ubiquitous Technologies* 6, 3 (2022), 1–28.
- [12] Sai Kumar Dwivedi, Yu Sun, Priyanka Patel, Yao Feng, and Michael J Black. 2024. TokenHMR: Advancing Human Mesh Recovery with a Tokenized Pose Representation. In *Proceedings of the IEEE/CVF Conference on Computer Vision and Pattern Recognition*. 1323–1333.
- [13] Jiawei Fang, Haishan Song, Chengxu Zuo, Xiaoxia Gao, Xiaowei Chen, Shihui Guo, and Yipeng Qin. 2024. SuDA: Support-based Domain Adaptation for Sim2Real Motion Capture with Flexible Sensors. *arXiv preprint arXiv:2405.16152* (2024).
- [14] Runyang Feng, Yixing Gao, Tze Ho Elden Tse, Xueqing Ma, and Hyung Jin Chang. 2023. DiffPose: SpatioTemporal diffusion model for video-based human pose estimation. In *Proceedings of the IEEE/CVF International Conference on Computer Vision*. 14861–14872.
- [15] Nima Ghorbani and Michael J Black. 2021. Soma: Solving optical marker-based mocap automatically. In *Proceedings of the IEEE/CVF International Conference on Computer Vision*. 11117–11126.
- [16] Harish Haresamudram, Irfan Essa, and Thomas Plötz. 2022. Assessing the state of self-supervised human activity recognition using wearables. *Proceedings of the ACM on Interactive, Mobile, Wearable and Ubiquitous Technologies* 6, 3 (2022), 1–47.
- [17] Jonathan Ho, Ajay Jain, and Pieter Abbeel. 2020. Denoising diffusion probabilistic models. *Advances in neural information processing systems* 33 (2020), 6840–6851.
- [18] S Zohreh Homayounfar and Trisha L Andrew. 2020. Wearable sensors for monitoring human motion: a review on mechanisms, materials, and challenges. *SLAS TECHNOLOGY: Translating Life Sciences Innovation* 25, 1 (2020), 9–24.
- [19] Yinghao Huang, Manuel Kaufmann, Emre Aksan, Michael J Black, Otmar Hilliges, and Gerard Pons-Moll. 2018. Deep inertial poser: Learning to reconstruct human pose from sparse inertial measurements in real time. *ACM Transactions on Graphics (TOG)* 37, 6 (2018), 1–15.
- [20] Yash Jain, Chi Ian Tang, Chulhong Min, Fahim Kawsar, and Akhil Mathur. 2022. Colloss: Collaborative self-supervised learning for human activity recognition. *Proceedings of the ACM on Interactive, Mobile, Wearable and Ubiquitous Technologies* 6, 1 (2022), 1–28.
- [21] Yifeng Jiang, Yuting Ye, Deepak Gopinath, Jungdam Won, Alexander W Winkler, and C Karen Liu. 2022. Transformer inertial poser: Real-time human motion reconstruction from sparse imus with simultaneous terrain generation. In *SIG-GRAPH Asia 2022 Conference Papers*. 1–9.
- [22] Fang Jiawei, Chengxu Zuo, Xiaoxia Gao, Xiaowei Chen, Shihui Guo, Yipeng Qin, et al. 2024. SuDA: Support-based Domain Adaptation for Sim2Real Hinge Joint Tracking with Flexible Sensors. In *Forty-first International Conference on Machine Learning*.
- [23] Abhi Kamboj and Minh Do. 2024. A Survey of IMU Based Cross-Modal Transfer Learning in Human Activity Recognition. *arXiv preprint arXiv:2403.15444* (2024).
- [24] Abhi Kamboj, Anh Duy Nguyen, and Minh Do. 2024. Fusion and Cross-Modal Transfer for Zero-Shot Human Action Recognition. *arXiv preprint arXiv:2407.16803* (2024).
- [25] Diederik P Kingma. 2013. Auto-encoding variational bayes. *arXiv preprint arXiv:1312.6114* (2013).
- [26] Ralf Kittler, Manfred Kayser, and Mark Stoneking. 2003. Molecular evolution of Pediculus humanus and the origin of clothing. *Current Biology* 13, 16 (2003), 1414–1417.
- [27] Kai Kunze and Paul Lukowicz. 2008. Dealing with sensor displacement in motion-based onbody activity recognition systems. In *Proceedings of the 10th international conference on Ubiquitous computing*. 20–29.
- [28] Wenhao Li, Hong Liu, Hao Tang, Pichao Wang, and Luc Van Gool. 2022. Mh-former: Multi-hypothesis transformer for 3d human pose estimation. In *Proceedings of the IEEE/CVF Conference on Computer Vision and Pattern Recognition*. 13147–13156.
- [29] Yunzhu Li and Yiyue Luo. 2024. Intelligent textiles are looking bright. *Science* 384, 6691 (2024), 29–30.
- [30] Ziwei Liao, Jialiang Zhu, Chunyu Wang, Han Hu, and Steven L. Waslander. 2024. Multiple View Geometry Transformers for 3D Human Pose Estimation. In *Proceedings of the IEEE/CVF Conference on Computer Vision and Pattern Recognition (CVPR)*. 708–717.
- [31] Jianjian Lin and Jie Song. 2023. Design of motion capture system in physical education teaching based on machine vision. *Soft Computing* (2023), 1–10.
- [32] Matthew Loper, Naureen Mahmood, Javier Romero, Gerard Pons-Moll, and Michael J Black. 2023. SMPL: A skinned multi-person linear model. In *Seminal Graphics Papers: Pushing the Boundaries, Volume 2*. 851–866.
- [33] Peng Lu, Tao Jiang, Yining Li, Xiangtai Li, Kai Chen, and Wenming Yang. 2024. RTMO: Towards High-Performance One-Stage Real-Time Multi-Person Pose Estimation. In *Proceedings of the IEEE/CVF Conference on Computer Vision and Pattern Recognition*. 1491–1500.
- [34] Yang Lu, Han Yu, Wei Ni, and Liang Song. 2023. 3D real-time human reconstruction with a single RGBD camera. *Applied Intelligence* 53, 8 (2023), 8735–8745.
- [35] Yiyue Luo. 2023. Intelligent Textiles for Physical Human-Environment Interactions. In *Adjunct Proceedings of the 36th Annual ACM Symposium on User Interface Software and Technology*. 1–5.
- [36] Yifei Luo, Mohammad Reza Abidian, Jong-Hyun Ahn, Deji Akinwande, Anne M Andrews, Markus Antonietti, Zhenan Bao, Magnus Berggren, Christopher A Berkey, Christopher John Bettinger, et al. 2023. Technology roadmap for flexible sensors. *ACS nano* 17, 6 (2023), 5211–5295.
- [37] Yiyue Luo, Yunzhu Li, Pratyusha Sharma, Wan Shou, Kui Wu, Michael Foshey, Beichen Li, Tomás Palacios, Antonio Torralba, and Wojciech Matusik. 2021. Learning human–environment interactions using conformal tactile textiles. *Nature Electronics* 4, 3 (2021), 193–201.
- [38] Yiyue Luo, Kui Wu, Andrew Spielberg, Michael Foshey, Daniela Rus, Tomás Palacios, and Wojciech Matusik. 2022. Digital fabrication of pneumatic actuators with integrated sensing by machine knitting. In *Proceedings of the 2022 CHI Conference on Human Factors in Computing Systems*. 1–13.
- [39] Naureen Mahmood, Nima Ghorbani, Nikolaus F Troje, Gerard Pons-Moll, and Michael J Black. 2019. AMASS: Archive of motion capture as surface shapes. In *Proceedings of the IEEE/CVF international conference on computer vision*. 5442–5451.
- [40] Dushyant Mehta, Oleksandr Sotnychenko, Franziska Mueller, Weipeng Xu, Mohamed Elgharib, Pascal Fua, Hans-Peter Seidel, Helge Rhodin, Gerard Pons-Moll, and Christian Theobalt. 2020. XNect: Real-time multi-person 3D motion capture with a single RGB camera. *Acm Transactions On Graphics (TOG)* 39, 4 (2020), 82–1.
- [41] Thomas B Moeslund, Adrian Hilton, and Volker Krüger. 2006. A survey of advances in vision-based human motion capture and analysis. *Computer vision and image understanding* 104, 2-3 (2006), 90–126.
- [42] Movella. 2024. Movella: Innovation in Motion Capture and Sensor Technology. <https://www.movella.com/>. Accessed: 2024-08-10.
- [43] Michael Muller, Lydia B Chilton, Anna Kantosalo, Charles Patrick Martin, and Greg Walsh. 2022. GenAICHI: generative AI and HCI. In *CHI conference on human factors in computing systems extended abstracts*. 1–7.
- [44] Anindya Nag, Subhas Chandra Mukhopadhyay, and Jürgen Kosel. 2017. Wearable flexible sensors: A review. *IEEE Sensors Journal* 17, 13 (2017), 3949–3960.
- [45] Noitom. 2024. Noitom: Motion Capture Systems and Solutions. <https://noitom.com/>. Accessed: 2024-08-10.
- [46] OpenAI. 2022. DALL-E 2: Creating Images from Text. <https://openai.com/dall-e-2>. Accessed: 2024-09-11.
- [47] OpenAI. 2023. ChatGPT: Optimizing Language Models for Dialogue. <https://openai.com/chatgpt>. Accessed: 2024-09-11.

- [48] OpenAI. 2024. DALL-E 3: The Next Generation of Image Generation. <https://openai.com/index/dall-e-3/>. Accessed: 2024-09-11.
- [49] Optitrack. 2024. OptiTrack - Motion Capture Systems. <https://www.optitrack.com/>. Accessed: 2024-08-10.
- [50] Enrica Papi, Yen Nee Bo, and Alison H McGregor. 2018. A flexible wearable sensor for knee flexion assessment during gait. *Gait & posture* 62 (2018), 480–483.
- [51] Chaitanya Patel, Zhouyingcheng Liao, and Gerard Pons-Moll. 2020. Tailornet: Predicting clothing in 3d as a function of human pose, shape and garment style. In *Proceedings of the IEEE/CVF conference on computer vision and pattern recognition*. 7365–7375.
- [52] Marco Pesavento, Yuanlu Xu, Nikolaos Sarafianos, Robert Maier, Ziyan Wang, Chun-Han Yao, Marco Volino, Edmond Boyer, Adrian Hilton, and Tony Tung. 2024. ANIM: Accurate Neural Implicit Model for Human Reconstruction from a single RGB-D image. In *Proceedings of the IEEE/CVF Conference on Computer Vision and Pattern Recognition*. 5448–5458.
- [53] Xin Qin, Yiqiang Chen, Jindong Wang, and Chaohui Yu. 2019. Cross-dataset activity recognition via adaptive spatial-temporal transfer learning. *Proceedings of the ACM on Interactive, Mobile, Wearable and Ubiquitous Technologies* 3, 4 (2019), 1–25.
- [54] Xavier Robert-Lachaine, Hakim Mecheri, Christian Larue, and André Plamondon. 2017. Accuracy and repeatability of single-pose calibration of inertial measurement units for whole-body motion analysis. *Gait & posture* 54 (2017), 80–86.
- [55] Olaf Ronneberger, Philipp Fischer, and Thomas Brox. 2015. U-net: Convolutional networks for biomedical image segmentation. In *Medical image computing and computer-assisted intervention—MICCAI 2015: 18th international conference, Munich, Germany, October 5–9, 2015, proceedings, part III 18*. Springer, 234–241.
- [56] Nitin Saini, Chun-Hao P Huang, Michael J Black, and Amir Ahmad. 2023. Smart-Mocap: Joint estimation of human and camera motion using uncalibrated RGB cameras. *IEEE Robotics and Automation Letters* 8, 6 (2023), 3206–3213.
- [57] J Luis Samper-Escudero, Aldo F Contreras-González, Manuel Ferre, Miguel A Sánchez-Urán, and David Pont-Esteban. 2020. Efficient multiaxial shoulder-motion tracking based on flexible resistive sensors applied to exosuits. *Soft robotics* 7, 3 (2020), 370–385.
- [58] Umme Sara, Morium Akter, and Mohammad Shorif Uddin. 2019. Image quality assessment through FSIM, SSIM, MSE and PSNR—a comparative study. *Journal of Computer and Communications* 7, 3 (2019), 8–18.
- [59] Karthika Sheeja Prakash, Erik Andersen, Vicky Chantal von Einem, Sabari Kannan Muthalagu, Priyank Agarwal, Hermann Otto Mayr, Michael Seidenstuecker, Nikolaus Rosenstiel, Shad Roundy, Peter Woias, et al. 2023. Design and implementation of a wearable system based on a flexible capacitive sensor, monitoring knee laxity. *Advanced Sensor Research* 2, 10 (2023), 2300058.
- [60] Soyong Shin, Juyong Kim, Eni Halilaj, and Michael J Black. 2024. Wham: Reconstructing world-grounded humans with accurate 3d motion. In *Proceedings of the IEEE/CVF Conference on Computer Vision and Pattern Recognition*. 2070–2080.
- [61] Qing Shuai, Zhiyuan Yu, Zhize Zhou, Lixin Fan, Haijun Yang, Can Yang, and Xiaowei Zhou. 2023. Reconstructing Close Human Interactions from Multiple Views. *ACM Transactions on Graphics (TOG)* 42, 6 (2023), 1–14.
- [62] Jiaming Song, Chenlin Meng, and Stefano Ermon. 2020. Denoising diffusion implicit models. *arXiv preprint arXiv:2010.02502* (2020).
- [63] Teslasuit. 2024. Teslasuit: Full-Body Haptic Feedback, Motion Capture, and Biometric Data Analysis. <https://teslasuit.io/>. Accessed: 2024-08-10.
- [64] Arash Vahdat, Karsten Kreis, and Jan Kautz. 2021. Score-based generative modeling in latent space. *Advances in neural information processing systems* 34 (2021), 11287–11302.
- [65] Vicon. 2024. Vicon: Motion Capture Systems. <https://www.vicon.com/>. Accessed: 2024-08-10.
- [66] Timo Von Marcard, Bodo Rosenhahn, Michael J Black, and Gerard Pons-Moll. 2017. Sparse inertial poser: Automatic 3d human pose estimation from sparse imus. In *Computer graphics forum*, Vol. 36. Wiley Online Library, 349–360.
- [67] Jindong Wang, Vincent W Zheng, Yiqiang Chen, and Meiyu Huang. 2018. Deep transfer learning for cross-domain activity recognition. In *proceedings of the 3rd International Conference on Crowd Science and Engineering*. 1–8.
- [68] Mark Weiser. 1991. The Computer for the 21 st Century. *Scientific american* 265, 3 (1991), 94–105.
- [69] Jian Wu and Roozbeh Jafari. 2018. Orientation independent activity/gesture recognition using wearable motion sensors. *IEEE Internet of Things Journal* 6, 2 (2018), 1427–1437.
- [70] Size Wu, Sheng Jin, Wentao Liu, Lei Bai, Chen Qian, Dong Liu, and Wanli Ouyang. 2021. Graph-based 3d multi-person pose estimation using multi-view images. In *Proceedings of the IEEE/CVF international conference on computer vision*. 11148–11157.
- [71] Yufei Xu, Jing Zhang, Qiming Zhang, and Dacheng Tao. 2022. Vitpose: Simple vision transformer baselines for human pose estimation. *Advances in Neural Information Processing Systems* 35 (2022), 38571–38584.
- [72] Yufei Xu, Jing Zhang, Qiming Zhang, and Dacheng Tao. 2023. Vitpose++: Vision transformer for generic body pose estimation. *IEEE Transactions on Pattern Analysis and Machine Intelligence* (2023).
- [73] Suhang Ye, Yingyi Zhang, Jie Hu, Liujuan Cao, Shengchuan Zhang, Lei Shen, Jun Wang, Shouhong Ding, and Rongrong Ji. 2023. DistilPose: Tokenized pose regression with heatmap distillation. In *Proceedings of the IEEE/CVF Conference on Computer Vision and Pattern Recognition*. 2163–2172.
- [74] Xinyu Yi, Yuxiao Zhou, Marc Habermann, Soshi Shimada, Vladislav Golyanik, Christian Theobalt, and Feng Xu. 2022. Physical Inertial Poser (PIP): Physics-aware Real-time Human Motion Tracking from Sparse Inertial Sensors. In *IEEE/CVF Conference on Computer Vision and Pattern Recognition (CVPR)*.
- [75] Xinyu Yi, Yuxiao Zhou, Marc Habermann, Soshi Shimada, Vladislav Golyanik, Christian Theobalt, and Feng Xu. 2022. Physical inertial poser (pip): Physics-aware real-time human motion tracking from sparse inertial sensors. In *Proceedings of the IEEE/CVF Conference on Computer Vision and Pattern Recognition*. 13167–13178.
- [76] Xinyu Yi, Yuxiao Zhou, and Feng Xu. 2021. Transpose: Real-time 3d human translation and pose estimation with six inertial sensors. *ACM Transactions on Graphics (TOG)* 40, 4 (2021), 1–13.
- [77] Xinyu Yi, Yuxiao Zhou, and Feng Xu. 2024. Physical Non-inertial Poser (PNP): Modeling Non-inertial Effects in Sparse-inertial Human Motion Capture. *arXiv preprint arXiv:2404.19619* (2024).
- [78] Yusuke Yoshiyasu. 2023. Deformable mesh transformer for 3d human mesh recovery. In *Proceedings of the IEEE/CVF Conference on Computer Vision and Pattern Recognition*. 17006–17015.
- [79] Yingxuan You, Hong Liu, Ti Wang, Wenhao Li, Runwei Ding, and Xia Li. 2023. Co-evolution of pose and mesh for 3d human body estimation from video. In *Proceedings of the IEEE/CVF International Conference on Computer Vision*. 14963–14973.
- [80] Tao Yu, Zerong Zheng, Kaiwen Guo, Pengpeng Liu, Qionghai Dai, and Yebin Liu. 2021. Function4d: Real-time human volumetric capture from very sparse consumer rgbd sensors. In *Proceedings of the IEEE/CVF conference on computer vision and pattern recognition*. 5746–5756.
- [81] Tianhong Catherine Yu, Peter He, Chi-Jung Lee, Cassidy Cheesman, Saif Mahmud, Ruidong Zhang, François Guimbretière, Cheng Zhang, et al. 2024. SeamPose: Repurposing Seams as Capacitive Sensors in a Shirt for Upper-Body Pose Tracking. *arXiv preprint arXiv:2406.11645* (2024).
- [82] Jianfeng Zhang, Yujun Cai, Shuicheng Yan, Jiashi Feng, et al. 2021. Direct multi-view multi-person 3d pose estimation. *Advances in Neural Information Processing Systems* 34 (2021), 13153–13164.
- [83] Runhua Zhang, Leheng Chen, Yuanda Hu, Yueyao Zhang, Jiayi Chen, Tianzhan Liang, Xiaohua Sun, and Qi Wang. 2023. Textile-Sensing Wearable Systems for Continuous Motion Angle Estimation: A Systematic Review. *International Journal of Human-Computer Interaction* (2023), 1–21.
- [84] Jiachen Zhao, Fang Deng, Haibo He, and Jie Chen. 2020. Local domain adaptation for cross-domain activity recognition. *IEEE Transactions on Human-Machine Systems* 51, 1 (2020), 12–21.
- [85] Bo Zhou, Daniel Geissler, Marc Faulhaber, Clara Elisabeth Gleiss, Esther Friederike Zahn, Lala Shakti Swarup Ray, David Gamarra, Vitor Fortes Rey, Sungho Suh, Sizhen Bian, et al. 2023. MoCaPose: Motion Capturing with Textile-integrated Capacitive Sensors in Loose-fitting Smart Garments. *Proceedings of the ACM on Interactive, Mobile, Wearable and Ubiquitous Technologies* 7, 1 (2023), 1–40.
- [86] Yuxiao Zhou, Marc Habermann, Ikhsanul Habibie, Ayush Tewari, Christian Theobalt, and Feng Xu. 2021. Monocular real-time full body capture with inter-part correlations. In *Proceedings of the IEEE/CVF Conference on Computer Vision and Pattern Recognition*. 4811–4822.
- [87] Chengxu Zuo, Jiawei Fang, Shihui Guo, and Yipeng Qin. 2023. Self-adaptive motion tracking against on-body displacement of flexible sensors. (2023).
- [88] Chengxu Zuo, Yiming Wang, Lishuang Zhan, Shihui Guo, Xinyu Yi, Feng Xu, and Yipeng Qin. 2024. Loose inertial poser: Motion capture with IMU-attached loose-wear jacket. In *Proceedings of the IEEE/CVF Conference on Computer Vision and Pattern Recognition*. 2209–2219.